THE JOURNAL OF PROSTHETIC DENTISTRY

RESEARCH AND EDUCATION

Effect of heating palladium-silver alloys on ceramic bond strength

Jie-yin Li, DDS,[a] Rui-nan Li, DDS,[b] Shao-hai Chang, DDS,[c] Pei-lin Zhuang, DDS,[d] Juan-kun Liao, DDS,[e] Xiu-hua Ye, DDS,[f] and Jian-tao Ye, DDS, MD[g]

ABSTRACT

Statement of problem. The effects of different heat treatments on the internal oxidation and metal–ceramic bond in Pd-Ag alloys with different trace elements require further documentation.

Purpose. The purpose of this in vitro study was to determine whether heat treatment affects the metal–ceramic bond strength of 2 Pd-Ag alloys containing different trace elements.

Material and methods. Thirteen cast specimens (25×3×0.5 mm) from each of 2 Pd-Ag alloy groups (W-1 and Argelite 61+3) were allocated to heat treatments before porcelain application: heating under reduced atmospheric pressure of 0.0014 MPa and 0.0026 MPa and heating under normal atmospheric pressure. Bond strengths were evaluated using a 3-point bending test according to ISO9693. Results were analyzed using 2-way ANOVA and Tukey HSD test (α=.05). Visual observation was used to determine the failure types of the fractured specimens. Scanning electron microscopy and energy dispersive spectroscopy were used to study morphologies, elemental compositions, and distributions in the specimens.

Results. The W-1 group had a mean bond strength significantly higher than that of Argelite 61+3 (P<.001). Heating under reduced atmospheric pressures of 0.0014 MPa and 0.0026 MPa resulted in similar bond strengths (P=.331), and both pressures had significantly higher bond strengths than that of heating under normal atmospheric pressure (P=.002, P<.001). Heating under different air pressures resulted in Pd-Ag alloys that contained either Sn or In and Ga, with various degrees of internal oxidation and different quantities of metallic nodules.

Conclusions. Heating under reduced atmospheric pressure effectively improved the bond strength of the ceramic-to-Pd-Ag alloys. (J Prosthet Dent 2015;114:715-724)

Although many studies have focused on developing and improving ceramic systems,[1] metal ceramic fixed prostheses are still important because of their versatility, their reasonable cost, and their lower clinical failure compared with ceramic fixed prostheses.[2] Pd-Ag alloys were introduced in the 1970s and were considered suitable for dental purposes.[3] The problematic green discoloration of porcelain by these alloys has been largely eliminated.[4] The alloys were developed to provide an alternative to more expensive Au-based alloys. Two types of Pd-Ag alloys have been marketed. One alloy contains approximately 60% palladium, 28% to 30% silver, indium, and tin, and other trace elements. The other alloy type has slightly less palladium (50%-55%) and more silver (35%-40%), tin, and other trace elements but little or no indium.[5] Indium and tin have also been helpful in improving the metal–ceramic bond.

The primary requirement for a successful metal ceramic restoration is a lasting bond between the ceramic and alloy. Four factors determine the success of a metal–ceramic bond: chemical bonding, mechanical bonding, van der Waals forces, and compressive forces.[6] Chemical bonding is considered the predominant factor

[a]Resident, Department of Prosthodontics, Sun Yat-sen Memorial Hospital, Sun Yat-sen University, Guangzhou, China; and Resident, Department of Stomatology, Jieyang People's Hospital, Jieyang, China.
[b]Technical Director, Dingyuan Dental Lab Ltd, Dongguan, China.
[c]Assistant Professor, Department of Prosthodontics, Sun Yat-sen Memorial Hospital, Sun Yat-sen University, Guangzhou, China.
[d]Resident, Department of Prosthodontics, Sun Yat-sen Memorial Hospital, Sun Yat-sen University, Guangzhou, China.
[e]Resident, Department of Prosthodontics, Sun Yat-sen Memorial Hospital, Sun Yat-sen University, Guangzhou, China.
[f]Resident, Department of Prosthodontics, Sun Yat-sen Memorial Hospital, Sun Yat-sen University, Guangzhou, China.
[g]Assistant Professor, Department of Prosthodontics, Sun Yat-sen Memorial Hospital, Sun Yat-sen University, Guangzhou, China.

Clinical Implications

Applying heat under reduced atmospheric pressure before porcelain application improved the bond strength between the ceramic and Pd-Ag alloys containing either Sn or In and Ga.

in the success of a metal-ceramic bond. However, controversy exists regarding the bonding mechanism between Pd-Ag alloys and ceramic. Some scientists believe that Pd-Ag alloys form internal rather than external oxides and that the nodules on the external surface of the metal alloy attributed to internal oxidation may provide more mechanical retention than chemical retention for the porcelain.[7,8] Others believe that the oxide film on the Pd-Ag alloy surface plays a leading role in porcelain adherence.[9,10]

Investigation of the high-temperature behavior of Pd-Ag-Sn-In alloy[7] showed that, after heating under reduced atmospheric pressures of 0.01 MPa, alloy surface nodules were formed by a Nabarro-Herring creep mechanism driven by the internal oxidation of tin and indium. Additionally, the quantity of metallic nodules increased as the temperatures increased. An internally oxidized layer rich in Sn was found beneath the alloy surfaces. No surface oxides were detected, and mechanical interlocking is considered the most important factor for porcelain adherence. Li et al[8] found that different quantities of Pd-Ag metallic nodules formed on the Sn-containing Pd-Ag alloy surface after 2 different heat treatments. An internally oxidized structure rich in Sn was observed at various depths beneath the surfaces. Shimizu et al[11] and Guo et al[12] found that Pd-Ag alloys with differing amounts of In, Ga, and Sn exhibited different physical and mechanical properties.

Several methods exist for evaluating metal-ceramic bond strength, including the shear,[13,14] biaxial flexure,[15] and 3-[16] and 4-point bend tests.[17] The 3-point bend test has been standardized by the ISO9693[18] as a metal-ceramic bond test.

To study the effect of heat treatment under various air pressures and with different trace elements in the alloys on the internal oxidation and metal-ceramic bond strength of Pd-Ag alloys, this study compared the internal oxidation and metal-ceramic bond strength of 2 Pd-Ag alloys containing either Sn or In and Ga after 3 different heat treatments. The null hypothesis was that the type of Pd-Ag alloy and heat treatment methods would not affect bond strength.

MATERIAL AND METHODS

The Pd-Ag alloys used in this study were W-1 (Ivoclar Vivadent AG) and Argelite 61+3 (Argen). Their elastic modulus values as provided by the manufacturer were 114 GPa and 120 GPa, respectively, and the compositions (wt%) provided by the manufacturer were 53.3 Pd, 37.7 Ag, 8.5 Sn, and <1.0 In, Ru, and Li for W-1; and 61 Pd, 23.35 Ag, 3 Au, 10 In, and 2.5 Ga for Argelite 61+3. The porcelain bonded to the alloys was Ceramco III (Dentsply Intl).

A 3-dimensional modeler (Projet-DP 3000; 3D Systems) was used to obtain 80 acrylic resin metal framework templates (VisiJet CP200; 3D Systems) (25×3×0.5 mm) according to ISO9693.[18] Each template was mounted in a silicone ring (Ugin) and then poured in investment material (Bellavest SH; Bego) according to the manufacturer's recommendations. W-1 and Argelite 61+3 Pd-Ag alloys (40 specimens each) were cast in an electrical induction furnace (Nautilus; Bego). Sprues were removed with silicon carbide disks at low speed, followed by airborne-particle abrasion with 110-μm Al_2O_3 particles to remove investment material. Dimensions of the cast specimens were measured with a digital caliper (HengLiang).

The specimen surfaces selected to receive the ceramics were airborne-particle abraded (S-605; Jialixing) from 1 cm and at 45 degrees with 250-μm Al_2O_3 for 10 seconds at 0.2 MPa. Specimens were cleaned ultrasonically in a distilled water bath (CD-4820; Kelin). Then, 1 metal specimen from each alloy was used for surface observation, using scanning electron microscopy (SEM; JCX8100; JEOL). Then, to examine the cross-sections of the metal layers, those specimens taken from each alloy were embedded in autopolymerizing acrylic resin (Weiyi Industrial Co, Ltd), and the section was ground and polished. Specimens were then ultrasonically cleaned, dried, and sprayed with carbon. SEM was used to observe the morphologies in cross-section.

The remaining 39 specimens of each alloy were divided by using a simple random method into 3 subgroups (n=13), according to the heat treatment type: heating under reduced atmospheric pressure of 0.0014 MPa or 0.0026 MPa or under normal atmospheric pressure. The specimens heated under normal atmospheric pressure were placed in a dental porcelain furnace (Programat P300; Ivoclar Vivadent AG) preheated to 600°C. The temperature was increased to 1010°C at 70°C/min and held for 5 minutes at the highest temperature according to the manufacturer's recommendations; the air pressure was maintained at standard atmospheric pressure (0.1 MPa). Specimens heated under reduced atmospheric pressure were heat treated using the same procedures, except that the air pressure in the furnace was reduced to 0.0014 MPa or 0.0026 MPa. After heat treatment, 1 metal specimen was taken from each group so that its surface and cross-section could be studied using SEM and energy dispersive spectroscopy (EDS) (Oxford-7412; Oxford Instruments) in the same

Table 1. Firing schedules of porcelains

Layer of Porcelain	Start Temperature (°C)	Preheat Time (min)	Heat Rate (°C/min)	Final Temperature (°C)	Holding Time (min)
First opaque layer	600	5	60	975	1
Second opaque layer	600	3	60	970	0
Dentin	600	5	60	930	1
Glaze	600	3	55	920	0.5

Vacuum level was 0.0014 MPa.

way as that for the metal specimens before heat treatment.

An 8.0×3.0×1.1-mm ceramic layer was applied to the central portion of the surface of each remaining metal specimen and fired in a furnace (Programat P300; Ivoclar Vivadent AG), following the manufacturer's recommendations (Table 1). One metal ceramic specimen was taken from each group so that the metal–ceramic interface with SEM and EDS could be studied in the same way as for the metal specimen cross-section.

The bond strength of the metal-ceramic specimens of each group (n=11) was determined from a 3-point bend test in a universal testing machine (SANS), according to the ISO9693 standard.[18] The debonding load (F_{fail}) for each specimen was recorded, and the metal-ceramic bond strength (τ_b) was calculated by using the formula $\tau_b = k \times F_{fail}$ (ISO9693).[18] The coefficient k depends on the alloy thickness and the elastic modulus of the metallic material. The alloy surfaces that had debonded from the porcelain were analyzed visually and with EDS to characterize the failure types. Failure types were classified as adhesive, along the interfacial region between the opaque ceramic and metal; cohesive, inside the ceramic; or a mixture of adhesive failure between the ceramic and metal with cohesive fracturing of the ceramic.[19]

Data for bond strength (MPa) were analyzed using 2-way ANOVA and Tukey HSD tests with the variables being "heat-treatment methods" and "alloy types" (α=.05).

RESULTS

Mean ±standard deviations of the bond strengths are shown in Table 2. Results for 2-way ANOVA (Table 3) showed that the mean bond strengths were affected significantly by alloy type (P<.001) and heat treatment method (P<.001). Interaction between the alloy type and heat treatment factors was not statistically significant (P=.620).

The Tukey test result demonstrated that, when the main factor alloy type was analyzed, W-1 (53.21 ±4.23 MPa) showed a significantly higher bond strength than Argelite 61+3 (49.26 ±3.53 MPa) (P<.001). When the main factor heat treatment was analyzed, the specimens that were heated under normal atmospheric pressure showed the lowest bond strength (48.37 ±3.37 MPa). This result was significantly different from that obtained by heating under reduced atmospheric pressures of 0.0026 MPa (53.39 ±4.25 MPa; P<.001) and 0.0014 MPa (51.95 ±3.90 MPa; P=.002). The 2 groups produced under reduced atmospheric pressures were not significantly different from each other (P=.331).

Table 2. Mean ±SD of bond strength (MPa) of 6 groups (n=11)

Heat Treatment Methods	Alloy Types	
	W-1	Argelite 61+3
Reduced atmospheric pressure of 0.0014 MPa	54.17 ±3.82	49.72 ±2.54
Reduced atmospheric pressure of 0.0026 MPa	55.69 ±3.54	51.08 ±3.71
Normal atmospheric pressure	49.78 ±3.08	46.97 ±3.16

Table 3. Results of 2-way ANOVA for alloy types, heat treatment methods, and their interactions

Effect	*df*	SS	MS	F	*P*
Alloy types	1	258.07	258.07	23.13	<.001*
Heat treatment methods	2	293.12	146.56	13.14	<.001*
Interaction	2	10.76	5.38	0.48	.620
Residue	60	669.48	11.16		
Total	66	174139.30			

df, degrees of freedom; F, F-statistic; MS, mean square; SS, sum of squares.
*Significance, P<.05.

Micrographs of the metal specimen surfaces are shown in Figure 1. No differences in morphology existed between the 2 alloys before heat treatment; both of the treatments exhibited a concave-convex surface from airborne-particle abrasion, and no metallic nodules were observed (Figs. 1A, 1B). Metallic nodules appeared on the specimen surfaces after various heat treatments. Heat treatments under higher air pressure resulted in a larger number of nodules on the Pd-Ag alloy surfaces. Nodules in the reduced atmospheric pressure groups were small and discrete and were dispersed randomly on the surface (Figs. 1C-1F). Nodules in the normal atmospheric groups were denser and coalesced into strips and blocks that almost entirely covered the 2 Pd-Ag alloy surfaces and weakened the original concave-convex surface appearance (Figs. 1G, 1H). Figure 2 shows photomicrographs of the metal specimen cross-section. The 2 alloys show uniform profile morphologies before heat treatment, with an irregular border at the top of the section created by airborne-particle abrasion (Figs. 2A, 2B). The metal specimens after heating show striped or banded structures beneath the surface. Higher air pressures resulted in a deeper extension of striped or banded structures beneath the surface (Figs. 2C-2H).

The elemental compositions of any nodular and non-nodular structures on the alloy surfaces after heat treatment were analyzed using EDS. Pd and Ag (Tables 4, 5) concentrated at the metallic nodules (Fig. 3A, 3B, spots 1 and 2) of the 2 Pd–Ag alloys. Pd, Ag, Sn, and O (Table 4) existed at the non-nodular region in the W-1 alloy

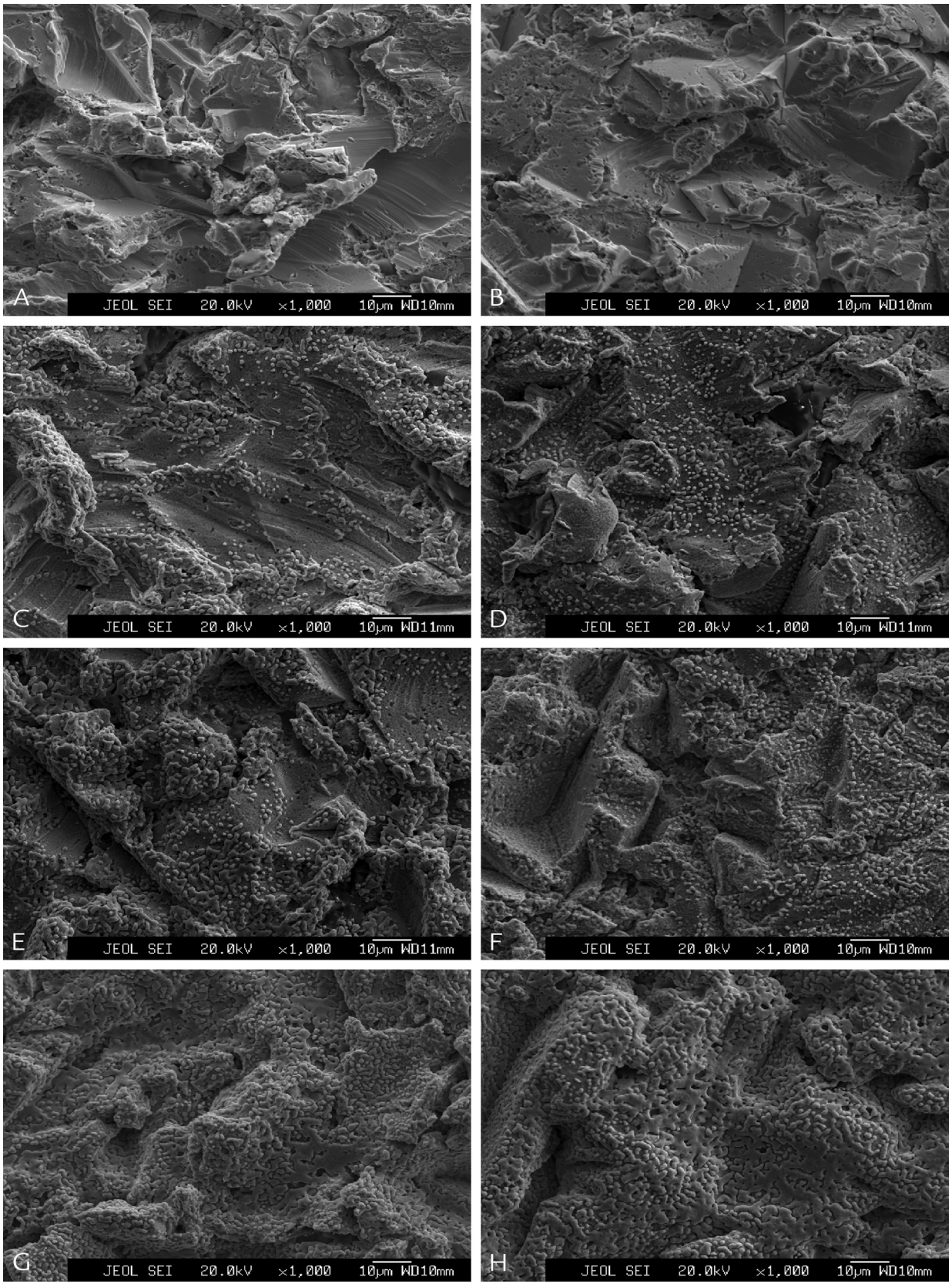

Figure 1. Surfaces of metal specimens (×1000). A, W-1 alloy before heat treatment. B, Argelite 61+3 alloy before heat treatment. C, W-1 alloy after heating at 0.0014 MPa. D, Argelite 61+3 alloy after heating at 0.0014 MPa. E, W-1 alloy after heating at 0.0026 MPa. F, Argelite 61+3 alloy after heating at 0.0026 MPa. G, W-1 alloy after heating under normal atmospheric pressure. H, Argelite 61+3 alloy after heating under normal atmospheric pressure.

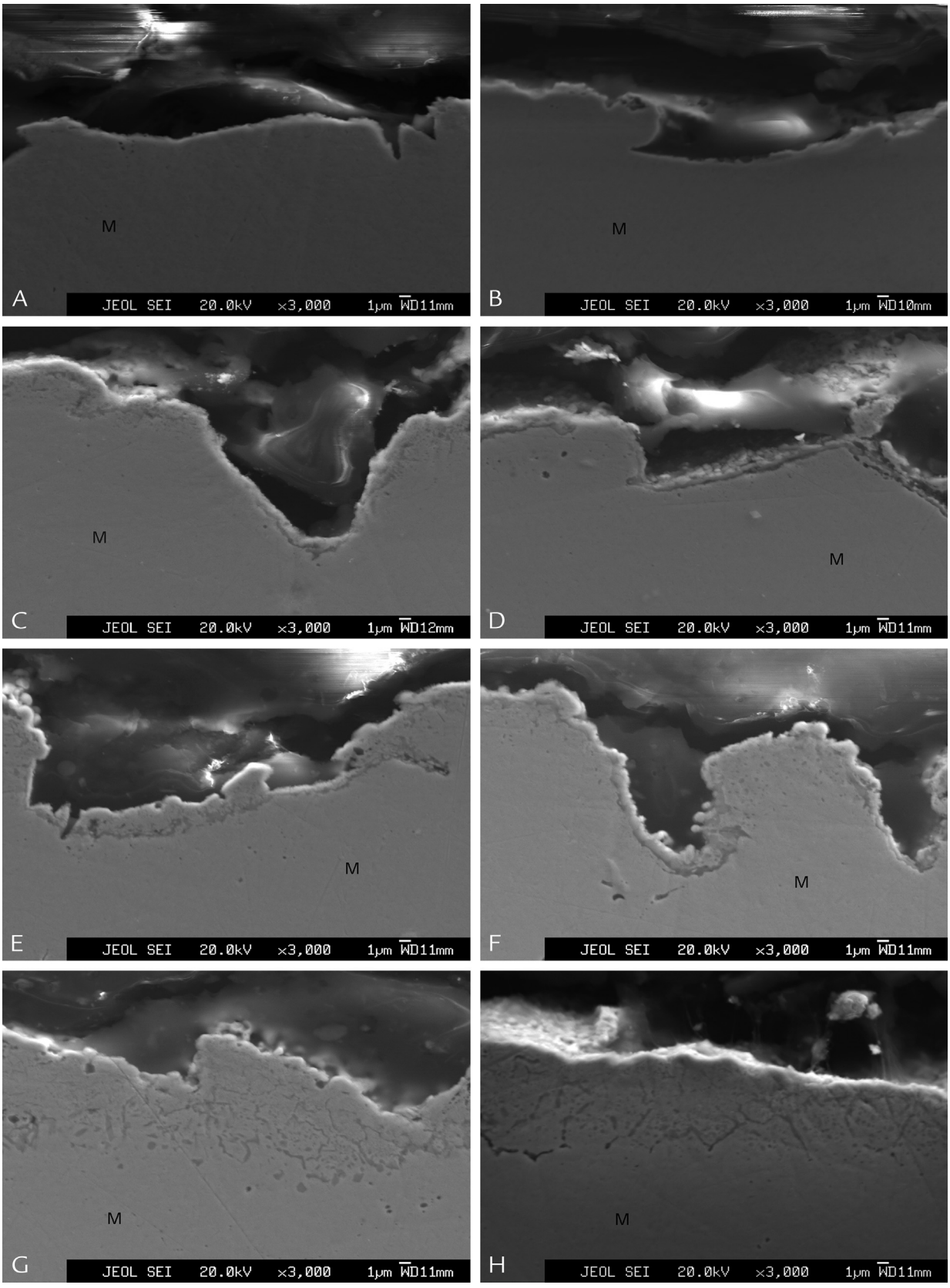

Figure 2. Cross-sections of metal specimens (×3000). A, W-1 alloy before heat treatment. M, metal. B, Argelite 61+3 alloy before heat treatment. C, W-1 alloy after heating at 0.0014 MPa. D, Argelite 61+3 alloy after heating at 0.0014 MPa. E, W-1 alloy after heating at 0.0026 MPa. F, Argelite 61+3 alloy after heating at 0.0026 MPa. G, W-1 alloy after heating under normal atmospheric pressure. H, Argelite 61+3 alloy after heating under normal atmospheric pressure.

Table 4. Elemental composition of W-1 alloy surface after heating at 0.0026 MPa by EDS analysis (wt%)

Spot*	O	Sn	Pd	Ag
1	–	–	55	45
2	–	–	50	50
3	24	27	28	21
4	19	27	29	25

EDS, energy dispersive spectroscopy.
*See Figure 3.

Table 5. Elemental composition of Argelite 61+3 alloy surface after heating at 0.0026 MPa by EDS analysis (wt%)

Spot*	O	In	Ga	Pd	Ag
1	–	–	–	56	44
2	–	–	–	56	44
3	18	23	10	26	23
4	15	33	8	24	20

EDS, energy dispersive spectroscopy.
*See Figure 3.

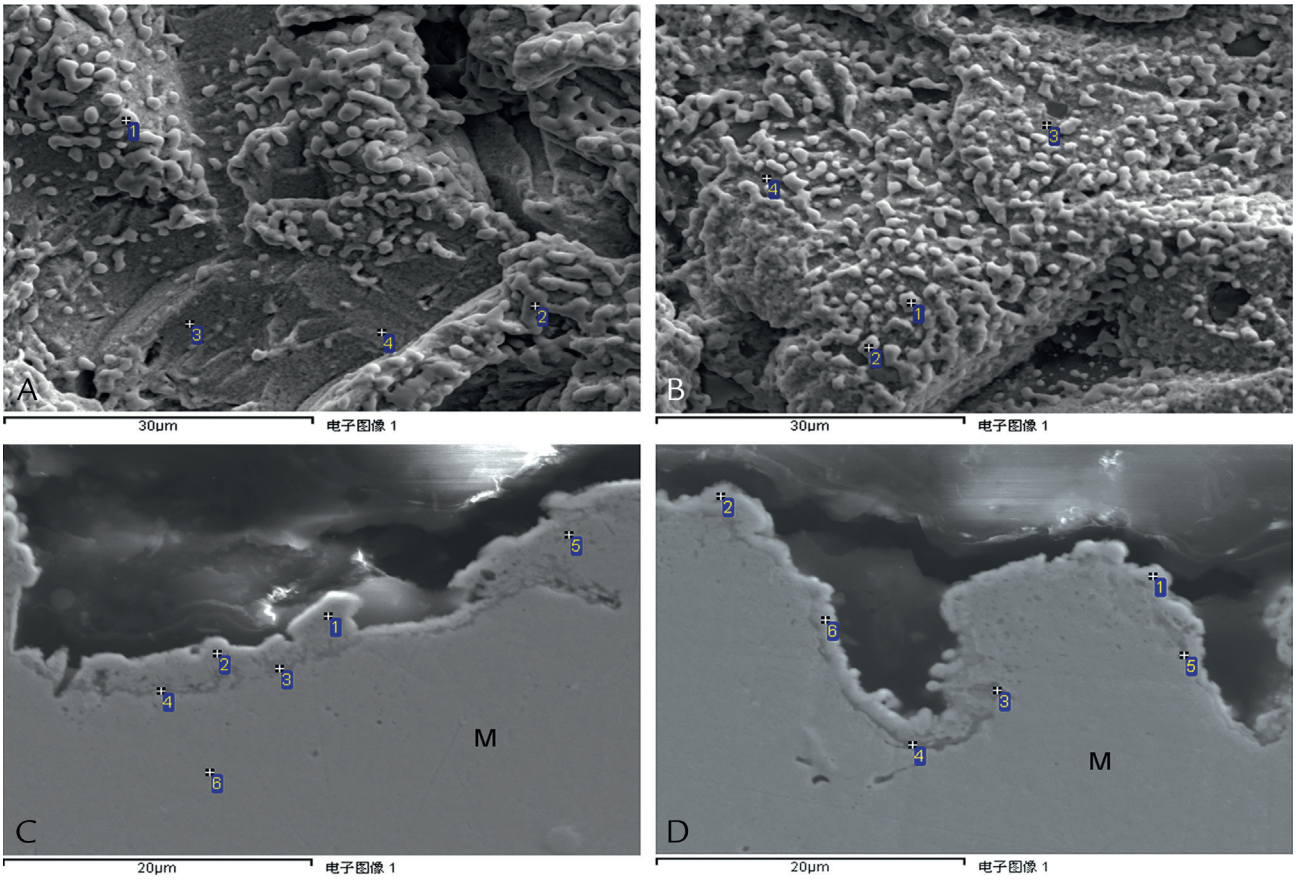

Figure 3. SEM imaging of metal specimen after heating at 0.0026 MPa. A, W-1 alloy surface. B, Argelite 61+3 alloy surface. C, W-1 alloy cross-section. D, Argelite 61+3 alloy cross-section. M, metal; SEM, scanning electron microscopy.

(Fig. 3A, spots 3 and 4), and the Sn and O amounts were much greater than that in the batch composition of the alloy. Pd, Ag, In, Ga, and O (Table 5) existed at the non-nodular region in the Argelite 61+3 alloy (Fig. 3B, spots 3 and 4), and the In, Ga, and O amounts were much greater than the batch composition of the alloy. EDS analysis showed that the cross-sectional striped structure was rich in Sn and O (Table 6) in the W-1 alloy (Fig. 3C, spots 3, 4, and 5) and in In, Ga, and O (Table 7) in the Argelite 61+3 alloy (Fig. 3D, spots 3, 4, and 5). These were the internal oxides of Sn, In, and Ga in the alloys.

Similar microscopic features of the metal-ceramic interface were observed in all groups. All interfaces were intact (no holes or slits), with good contact and wettability between the ceramic and the Pd-Ag alloy surfaces. The internally oxidized striped structures were similar to those of the cross-sections of the metal specimens after heat treatment (Fig. 4). The interfacial elemental compositions were studied using EDS. The internally oxidized layer was rich in Sn and O in the W-1 alloy (Fig. 5A, spots 2 and 3) and in In, Ga, and O in the Argelite 61+3 alloy (Fig. 5B, spots 2 and 3). The main elements present at the metal-ceramic interface (Figs. 5A, 5B, spots 5 and 6) were O, Si, Sn, Al, Na, K, Ca, and Ti. Sn and O concentrated at the grainy structure of the interface (Figs. 5A, 5B, spot 4).

Visual inspection showed that the failure type was mixed for all specimens and that the amount of ceramic

Table 6. Elemental composition of W-1 alloy section after heating at 0.0026 MPa by EDS analysis (wt%)

Spot*	O	Sn	Pd	Ag
1	–	–	49	51
2	4	10	42	44
3	32	45	12	11
4	29	35	18	18
5	25	36	20	19
6	–	9	63	28

EDS, energy dispersive spectroscopy.
*See Figure 3.

Table 7. Elemental composition of Argelite 61+3 alloy section after heating at 0.0026 MPa by EDS analysis (wt%)

Spot*	O	In	Ga	Pd	Ag
1	–	13	4	45	38
2	5	10	2	44	39
3	26	40	13	12	9
4	33	39	12	9	7
5	29	35	10	14	12
6	–	9	3	62	26

EDS, energy dispersive spectroscopy.
*See Figure 3.

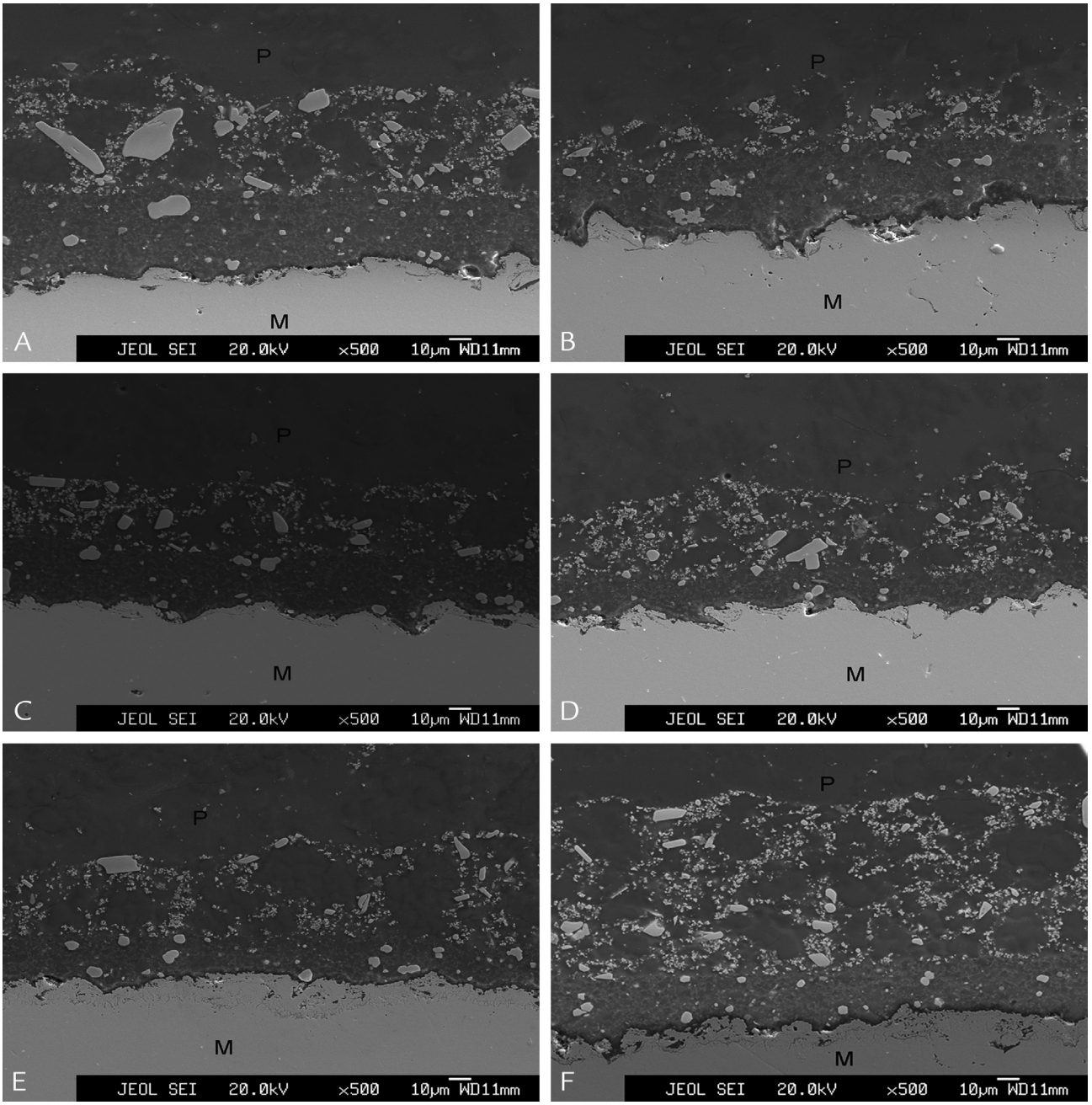

Figure 4. Interfaces of metal ceramic specimens (×500). A, W-1 alloy after heating at 0.0014 MPa. M, metal; P, porcelain. B, Argelite 61+3 alloy after heating at 0.0014 MPa. C, W-1 alloy after heating at 0.0026 MPa. D, Argelite 61+3 alloy after heating at 0.0026 MPa. E, W-1 alloy after heating under normal atmospheric pressure. F, Argelite 61+3 alloy after heating under normal atmospheric pressure.

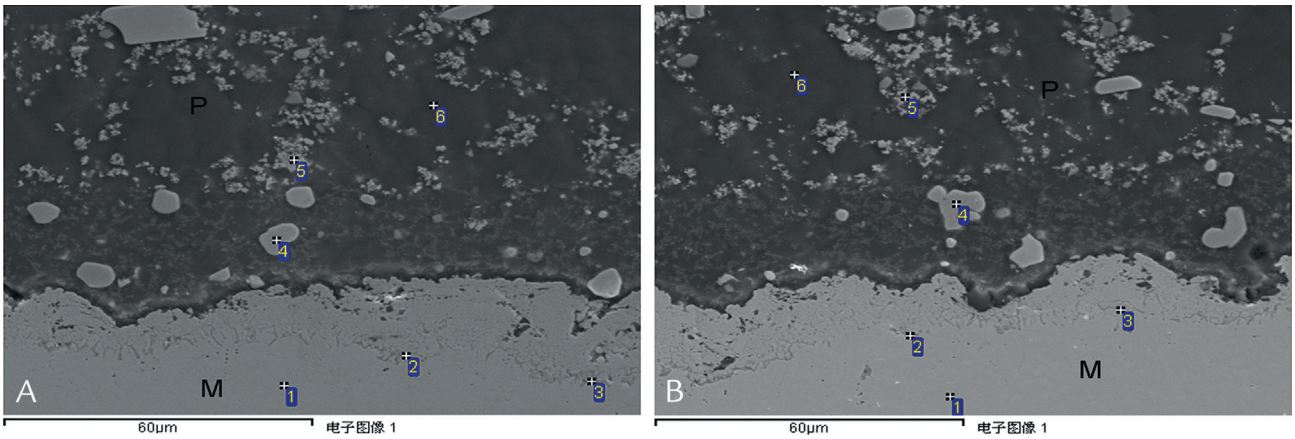

Figure 5. SEM imaging of metal–ceramic interfaces heat treated under normal atmospheric pressure. A, W-1 alloy. B, Argelite 61+3 alloy. M, metal; P, porcelain; SEM, scanning electron microscopy.

remaining on the porcelain-debonded metal surface differed among specimens. As Figure 6 shows, the porcelain-debonded metal surface in the 2 reduced atmospheric pressure groups had the largest residual ceramic area. Residual ceramic was thick and massive, with an irregular surface, whereas the ceramic layer of the specimens in the normal atmospheric groups mostly blocked exfoliation, and the residual ceramic was small and point-like, with a relatively smooth surface. The gray areas on the porcelain-debonded metal surface indicated that the Pd-Ag substrate, in which the main elemental Pd and Ag compositions were detected by EDS, represented an adhesive failure along the metal–ceramic interface. The light yellow areas on the porcelain-debonded metal surface (Fig. 6) show the remaining porcelain, in which the main elements O, Na, Al, Si, K, Ti, and Sn were detected by EDS, implying the existence of a cohesive fracture within the porcelain.

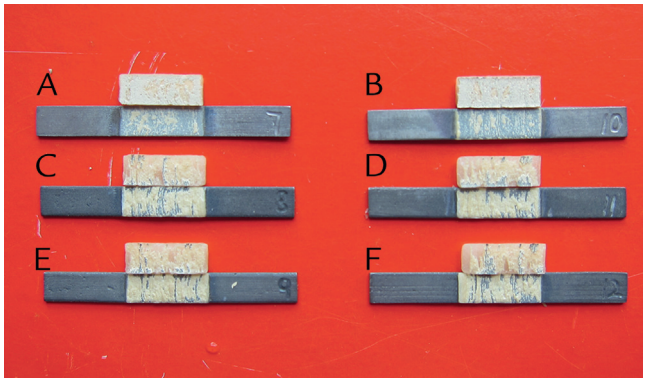

Figure 6. Macroscopic views of fractured specimens. A, W-1 alloy after heating under normal atmospheric pressure. B, Argelite 61+3 alloy after heating under normal atmospheric. C, W-1 alloy after heating at 0.0014 MPa. D, Argelite 61+3 alloy after heating at 0.0014 MPa. E, W-1 alloy after heating at 0.0026 MPa. F, Argelite 61+3 alloy after heating at 0.0026 MPa.

DISCUSSION

This study evaluated the metal-ceramic bond strength of 2 Pd-Ag alloys after 3 different heat treatments and found that both the type of Pd-Ag alloy and the heat treatment method significantly affected bond strength. Thus, the null hypothesis was rejected.

Metal–ceramic thermal compatibility is important in fabricating metal–ceramic restorations. Usually, the coefficient of thermal expansion (CTE) of the alloy is higher than that of the ceramic, and a variation from 0.5 to 1.0×10^{-6}/°C is considered adequate.[20] The CTE of Ceramco III used in this study has a wide application range, and the CTEs were 15.2×10^{-6}/°C for W-1 and 14.5×10^{-6}/°C for Argelite 61+3 alloys. Both of the metals used in this study were considered thermally compatible with porcelain and are commonly matched in clinical use. The bond strength values of all groups from our study (ranging from 46.97 ±3.16 MPa to 55.69 ±3.54 MPa) matched those from a study conducted by Li et al[8] (a range from 45.00 ±3.63 MPa to 51.61 ±5.91 MPa). However, the metal–ceramic bond strength was just one of the factors for the strength of a metal ceramic restoration; the strength of the metal framework and differences in CTE between metal and porcelain may also be factors. Differences in bond strength, therefore, are not entirely representative of clinical performance.

As indicated by EDS analysis, Pd and Ag, rather than oxides, accumulated at the surface metallic nodular structures of the 2 Pd-Ag alloys after heat treatment, but the non-nodular structures showed large amounts of Sn and O in the W-1 alloy and Ga, In, and O in the Argelite 61+3 alloy; oxides therefore formed on the non-nodular structure. The surfaces of the 2 alloys were covered almost entirely with coalesced nodules in the normal atmospheric pressure groups. The area of the non-nodular structure was small, which suggests that little or no oxide formed on

the surface. However, in the 2 reduced atmospheric pressure groups, the area of the non-nodular structure on the surface of the 2 alloys was much larger, and a large amount of oxides formed on the surface. Limkool and Sumii[21] also found that In_2O_3 and Ga_2O_3 formed on the Pd-Ag alloy surface after heating under reduced atmospheric pressure. The surface oxides in the reduced atmospheric pressure groups provide the basis for the chemical bond. The surface-coalesced nodule in the normal atmospheric pressure groups reduced the surface oxide significantly and weakened the original concave-convex surface appearance, resulting in a simultaneously adverse impact on the chemical and mechanical bonds. Li et al[8] confirmed that the Pd-Ag alloy has a rougher surface appearance after heating under reduced atmospheric pressure than that after heating under normal atmospheric pressure, under the same airborne-particle abrasion conditions. This study also found that a larger amount of residual ceramic remained on the surface of the porcelain-debonded metal in the 2 reduced atmospheric pressure groups. These findings may explain why the bond strengths of the reduced atmospheric pressure groups were higher than those of the normal atmospheric pressure groups.

According to internal oxidation theory,[7] Pd-Ag alloys dissolve substantial quantities of oxygen at elevated temperature. The volume of nodular material on the alloy surface is equal to the volume increase because of the internal oxidation of Sn and In. The formation of nodules relieves the dilational stresses developed when the dissolved tin and indium in the Pd-Ag solid solution was converted to oxide. The molar volume of SnO_2 is 60% greater than that of Sn in solid solution, and the formation of In_2O_3 results in a 48% increase in volume over In. The movement of internal oxidation may be accelerated, slowed, halted, or reversed by altering the temperature or air pressure. In this study, similar internal oxidation after heat treatment was observed on the Pd-Ag alloys containing either Sn or Ga and In. The degree of internal oxidation depends on the air pressure in heat treatment. A higher air pressure results in a higher number of metallic nodules on the surface, internal Sn or In oxides beneath the surface, and less oxide on the surface. The internally oxidized structures of the metal ceramic specimens remained similar to those of the metal specimens after heat treating, though multiple sintering of porcelain occurred. The composition of Ga in Argelite 61+3 is 2.5 (wt%). A few internal Ga oxides were detected beneath the surface in this study. However, in the Pd-Cu-Ga and Pd-Ga alloys, which contain more Ga, an internally oxidized layer showed large amounts of gallium oxide.[22]

We compared the quantity of nodules on the Pd-Ag alloy surface after heating at the same temperature but with different air pressures. Fewer nodules existed on the surface after heat treatment at 0.0014 MPa than at 0.0026 MPa, and the quantity of nodules after heat treatment at 0.0026 MPa was similar to that at 0.0036 MPa in a study conducted by Li et al.[8] However, Mackert et al[7] found that approximately 95% of the Pd-Ag alloy surface was covered with coalesced nodules after heat treatment at 0.01 MPa. This result is similar to that after heat treatment under normal atmospheric pressure (0.1 MPa) in this study. It is reasonable for the Pd-Ag alloy to be heat treated at a lower atmospheric pressure (less than 0.0036 MPa). The atmospheric pressure and nodular coverage for obtaining the highest bond strength requires further research.

One limitation of this study was the use of visual examination to assess the failure types, and a future study using the Si line of EDS to provide more desirable information about the amount of residual ceramic is needed.

CONCLUSIONS

Within the limitations of this study, it can be concluded that heating under reduced atmospheric pressure before ceramic application improved the bond strength between the ceramic and the Pd-Ag alloys. The degree of internal oxidation of the Pd-Ag alloys containing either Sn, or In and Ga is related to the air pressure in heat treatment.

REFERENCES

1. Joias RM, Tango RN, de Araujo JEJ, de Araujo MAJ, de Siqueira Ferreira Anzaloni Saavedra G, de Arruda Paes-Junior TJ, et al. Shear bond strength of a ceramic to Co-Cr alloys. J Prosthet Dent 2008;99:54-9.
2. Vojdani M, Shaghaghian S, Khaledi A, Adibi S. The effect of thermal and mechanical cycling on bond strength of a ceramic to nickel-chromium (Ni-Cr) and cobalt-chromium (Co-Cr) alloys. Indian J Dent Res 2012;23:509-13.
3. Goodacre CJ. Palladium–silver alloys: a review of the literature. J Prosthet Dent 1989;62:34-7.
4. Stavridakis MM, Papazoglou E, Seghi RR, Johnston WM, Brantley WA. Effect of different high-palladium metal–ceramic alloys on the color of opaque and dentin porcelain. J Prosthet Dent 2004;92:170-8.
5. Roberts HW, Berzins DW, Moore BK, Charlton DG. Metal–ceramic alloys in dentistry: a review. J Prosthodont 2009;18:188-94.
6. Bagby M, Marshall SJ, Marshall GW Jr. Metal-ceramic compatibility: a review of the literature. J Prosthet Dent 1990;63:21-5.
7. Mackert JR, Ringle RD, Fairhurst CW. High-temperature behavior of a Pd–Ag alloy for porcelain. J Dent Res 1983;62:1229-35.
8. Li BH, Ye JT, Liao JK, Zhuang PL, Zhang YP, Li JY. Effect of pretreatments on the metal-ceramic bonding strength of a Pd–Ag alloy. J Dent 2014;42:319-28.
9. Schweitzer DM, Goldstein GR, Ricci JL, Silva NR, Hittelman EL. Comparison of bond strength of a pressed ceramic fused to metal versus feldspathic porcelain fused to metal. J Prosthodont 2005;14:239-47.
10. Johnson T, van Noort R, Stokes CW. Surface analysis of porcelain fused to metal systems. Dent Mater 2006;22:330-7.
11. Shimizu T, Goto S, Oqura H. Effects of Sn, Ga, and In additives on properties of Ag-Pd-Au-Cu alloy for ultra-low fusing ceramics. Dent Mater J 2001;20:286-304.
12. Guo WH, Brantley WA, Li D, Clark WA, Monaghan P, Heshmati RH. Annealing study of palladium–silver dental alloys: Vickers hardness measurements and SEM microstructural observations. J Mater Sci Mater Med 2007;18:111-8.
13. Scolaro JM, Pereira JR, do Valle AL, Bonfante G, Pegoraro LF. Comparative study of ceramic-to-metal bonding. Braz Dent J 2007;18:240-3.
14. Lombardo GH, Nishioka RS, Souza RO, Michida SM, Kojima AN, Mesquita AM, et al. Influence of surface treatment on the shear bond strength of ceramics fused to cobalt-chromium. J Prosthodont 2010;19:103-11.

15. Sadeq A, Cai Z, Woody RD, Miller AW. Effects of interfacial variables on ceramic adherence to cast and machined commercially pure titanium. J Prosthet Dent 2013;90:10-7.
16. Yao L, Peng C, Wu J. Wettability and bond strength between leucite-reinforced dental porcelains and Co-Cr alloy. J Prosthet Dent 2013;110: 515-20.
17. Jochen DG, Caputo AA, Matyas J. Effect of opaque porcelain application on strength of bond to silver-palladium alloys. J Prosthet Dent 1990;63:414-8.
18. International Organization for Standardization. ISO 9693:1999(E). Metal–ceramic dental restorative systems. Available at: http://www.iso.ch/iso/en/prods-services/ISOstore/store.html. Accessed October 12, 2013.
19. Oliveira de Vasconcellos LG, Silva LH, Reis de Vasconcellos LM, Balducci I, Takahashi FE, Bottino MA. Effect of airborne- particle abrasion and mechanic-thermal cycling on the flexural strength of glass ceramic fused to gold or cobalt-chromium alloy. J Prosthodont 2011;20:553-60.
20. Wataha JC. Alloys for prosthodontic restorations. J Prosthet Dent 2002;87: 351-63.
21. Limkool P, Sumii T. Study of a Pd–Ag-Sb system alloy for metal–ceramics. Bulletin of Tokyo Dent Coll 1995;36:103-14.
22. Papazoglou E, Brantley WA, Mitchell JC, Cai Z, Carr AB. New high-palladium casting alloys: studies of the interface with porcelain. Int J Prosthodont 1996;9:315-22.

Corresponding author:
Dr Jian-tao Ye
Sun Yat-Sen Memorial Hospital
Sun Yat-Sen University
107 Yan-jiang Rd
510120 Guangzhou
CHINA
Email: dutaoye@163.com

Acknowledgments
The authors thank Dr Chao-qun Wu for assistance with specimen analysis and Dr Tian-xin Lin for expert advice and assistance with the manuscript preparation.